Research article

DPY30 knockdown suppresses colorectal carcinoma progression via inducing Raf1/MST2-mediated apoptosis

HaiFeng Jiang [a,b,1], WeiChao Su [a,g,1], HaiXing Wang [c,1], ChunYing Luo [d,1], YaTao Wang [a], LinJun Zhang [e], LingTao Luo [a], ZeBin Lu [f], DongYan Shen [e,**], GuoQiang Su [a,d,f,*]

[a] *Department of Colorectal Tumor Surgery, The First Affiliated Hospital of Xiamen University, School of Medicine, Xiamen University, Xiamen, 361003, Fujian Province, China*
[b] *Department of Critical Care Medicine, Second People's Hospital of Yibin City, Yibin, 644000, Sichuan Province, China*
[c] *Department of Endoscopy Center, The First Affiliated Hospital of Xiamen University, Xiamen, 361003, China*
[d] *Department of Pathology, Affiliated Hospital of Youjiang Medical University for Nationalities, Baise, 533000, China*
[e] *Xiamen Cell Therapy Research Center, The First Affiliated Hospital of Xiamen University, School of Medicine, Xiamen University, Xiamen, 361003, China*
[f] *Department of Clinical Medicine, Fujian Medical University, Fuzhou, 350122, China*
[g] *Xiamen Xianyue Hospital, Xianyue Hospital Affiliated with Xiamen Medical College, Fujian Psychiatric Center, Fujian Clinical Research Center for Mental Disorders, Xiamen, 361012, China*

A R T I C L E   I N F O

A B S T R A C T

Colorectal Carcinoma (CRC) is one of the most common malignant tumors of the digestive tract, with a high mortality rate. DPY30 is one of the core subunits of the histone methyltransferase complex, which was involved in many cancer processes. However, the role of DPY30 in the occurrence and progression of CRC remains unclear. In this study, we sought to evaluate the role and mechanism of DPY30 in CRC cells apoptosis. Here, we identified that knockdown of DPY30 significantly inhibited the HT29 and HCT116 cells proliferation *in vitro*. Moreover, the knockdown of DPY30 significantly increased the apoptosis rate and promoted the expression of apoptosis-related proteins in CRC cells. Meanwhile, DPY30 knockdown promoted CRC cells apoptosis through endogenous programmed death and in a caspase activation-dependent manner. Furthermore, RNA-seq analysis revealed that the action of DPY30 is closely related to the apoptosis biological processes, and screened its potential effectors Raf1. Mechanistically, DPY30 downregulation promotes MST2-induced apoptosis by inhibiting Raf1 transcriptional activity through histone H3 lysine 4 trimethylation (H3K4me3). *In vivo* experiments showed that DPY30 was correlated with Raf1 in nude mouse subcutaneous xenografts tissues significantly. Clinical colorectal specimens further confirmed that overexpression of DPY30 in malignant tissues was significantly correlated with Raf1 level. The vital role of the DPY30/Raf1/MST2 signaling axis in the cell death and survival rate of CRC cells was disclosed, which provides potential new targets for early diagnosis and clinical treatment of CRC.

  * Corresponding author. Department of Colorectal Tumor Surgery, The First Affiliated Hospital of Xiamen University, School of Medicine, Xiamen University, Xiamen, 361003, Fujian Province, China.
  ** Corresponding author.
    E-mail addresses: shendongyan@xmu.edu.cn (D. Shen), suguoqiang@xmu.edu.cn (G. Su).
  [1] These authors contributed equally to this work and share first authorship.

1. Introduction

Colorectal Carcinoma (CRC) attained a significant milestone in 2020, ranking as the third most prevalent cancer globally and the second leading cause of cancer-related mortality. During that year, there were 1,931,590 new CRC cases and 935,173 deaths cases reported, representing 10 % of all cancer cases and 9.4 % of global cancer-related deaths [1]. Moreover, projections indicate a worrisome trend, with an estimated annual increase to approximately 2.2 million new cases and 1.1 million deaths by 2030 [2]. While several therapies can improve the overall survival of advanced CRC, e.g., surgery, radiotherapy, chemotherapy, and immunotherapy, the effects are less than optimal [3]. Several of these therapeutic modalities are ultimately achieved by inducing CRC cells death, and apoptosis is one of the important modes of cell death, such as the apoptosis of CRC cells induced by the action of chemotherapy drugs docetaxel and cisplatin and HOXA-AS2 [4] oncogene knockdown. Therefore, it is of great significance to inhibit the occurrence and development of CRC by interfering with the proliferation/death pathway of CRC cells. Taken together, it is a long-awaited problem to find an effective treatment strategy for CRC patients, especially exploring novel therapeutic targets related to CRC cell death, which may contribute to the clinical diagnosis and treatment of malignant tumors.

In recent years, a growing body of evidence suggests that dysregulated epigenetic regulatory processes play an important role in cancer occurrence and progression [5–7]. Histone methyltransferases (HMT) are a class of enzymes that catalyze histone methylation and play a key role in the dynamic regulation of chromatin functions such as gene transcriptional regulation, chromatin stability, DNA damage and repair [8,9]. The SET1/MLL family complex, which belongs to HMT, is the most prominent H3K4 methyltransferase in mammals. These H3K4 methyltransferases (H3K4MT) enzymes contain distinct catalytic subunits with a common multisubunit core component, including WDR5, RBBP5, ASH2L, and DPY30, also known as WRADs [10–13]. Moreover, three different levels (mono-, di-, tri-) of methylation (me1, me2, me3) at H3K4 marked active and poised enhancers, gene bodies and transcription start sites, respectively [14,15].

DPY30 belongs to a core subunit of the human SET1/MLL complex and is essential for SET1/MLL methyltransferase activity [16, 17]. DPY30 and its homologs were mainly localized in the nucleus of cells; they are conserved in yeast, *Caenorhabditis elegans*, and humans [18], and regulates MLL complex to promote three levels of H3K4 methylation *in vitro* [19]and in yeast [20], zebrafish, mouse and human cells [17,21]. Recently, it has been found that DPY30 knockdown resulted in a global decrease of H3K4me3 [22], and regulate the normal proliferation and differentiation of hematopoietic progenitor cells [17] and is closely related to the differentiation potential of embryonic stem cells [16]. Furthermore, DPY30 could induce a senescent phenotype by affecting the expression of cell cycle-related factors p16 (CDKN2A) and p15 (CDKN2B), suggesting that DPY30 plays a pivotal role in regulating cellular senescence [22]. Epigenetic regulation of DPY30 has been reported to be a complex network of multiple molecular interactions including transcription factors, miRNAs and protein interactions. These regulatory mechanisms work together to influence the expression and function of DPY30, which in turn affects the methylation modification of histone H3 and processes such as gene expression, cell differentiation and development. Through the regulation of these regulatory mechanisms, DPY30 can be involved in the regulation of a variety of biological processes, including tumorigenesis and development, cardiac development and erythroid differentiation. Although the role of DPY30 in many cancers has been studied, its role and mechanism in CRC are not clearly understood.

In recent years, increasing evidences have shown that DPY30 is associated with tumor cell proliferation, invasion and metastasis [23–27]. Previous research shows that overexpression of DPY30 promotes CRC cell proliferation and cell cycle progression by facilitating the transcription of PCNA, Ki67 and cyclin A2 via mediating H3K4me3 [27]. However, the relationship between DPY30 and cell apoptosis and even whether it could mediate CRC tumorigenesis and development by regulating apoptosis remain unclear. Therefore, in this study, we used lentivirus-mediated shRNA to down-regulate the expression of DPY30 in the CRC cell line to identify the correlation between DPY30 and apoptosis and its regulatory effect on apoptosis. Furthermore, screened out the regulatory effector Raf1, and investigated the effect of DPY30 on the transcriptional expression of *Raf1* gene by affecting histone methylation modification, and clarified the molecular mechanism of DPY30 regulating Raf1/MST2 signaling axis to mediate CRC cell apoptosis. This study provided new insights into the function of DPY30 in CRC cells. We can better understand the downstream target genes and pathways that are affected by epigenetic effects regulated by DPY30, and new theoretical and experimental basis for the pathogenesis of colorectal carcinoma was presented.

2. Materials and methods

2.1. Chemicals and reagents

Dulbecco's modified Eagle's medium (DMEM) and Trypsin (with EDTA) were obtained from Gibco (Thermo Fisher Scientific, USA). Penicillin-streptomycin was obtained from BasalMedia. The radioimmunoprecipitation assay (RIPA) buffer supplemented with Phenylmethanesulfonyl fluoride (PMSF) was purchased from Solarbio (Beijing, China). Phosphatase and protease inhibitors were supplied by Roche Diagnostics (Shanghai, China). The primary antibodies used for WB and IHC included: DPY30 (ABclonal, A17796), Raf1 (Proteintech, 26863-1-AP). And other antibodies applied to WB as follows: GAPDH (CST, D16H11,#5714S), Bax (Proteintech, 60267-1-Ig), Bcl2 (Santa Cruz, sc-7382), Caspase-3 (CST, D3R6Y, #14220S), Cleaved Caspase-3 (CST, D175, #9661T), PARP (CST, 46D11, #9532S), YAP (CST, D8H1X, #14074S), p-YAP (CST, S127, #4911S), MST2 (PTM BIO, PTM-5408), p-MST2(CST, E7U1D, #49332), H3K4me3 (CST, C42D8, #9751S), Histone H3 (CST, D1H2, #4499S), Anti-mouse or rabbit secondary antibodies were purchased from Sigma. Other relevant kits or special supplies will be described below.

2.2. Cell culture and cell lines

The HCT116 and HT29 cell lines was donated by Professor Qingxi Chen from College of Life Sciences, Xiamen University (Xiamen, China). The cell lines were cultured in normal conditions with culturing medium DMEM containing 10 % (v/v) fetal bovine serum (FBS) and 1 % antibiotic (100 IU/ml of penicillin, 100 μg/ml of streptomycin). Furthermore, the cells were grown in an incubator with conditions of 5 % CO_2 and 37 °C. In all experiments of this study, cells were passaged every 48–72 h and were in the logarithmic phase.

2.3. Patients and tumor specimens

Colorectal cancer tissues and adjacent normal tissues were obtained during surgery and immediately cryopreserved in liquid nitrogen and soaked in 10 % neutral formaldehyde. All tissue specimens were obtained from the Department of Colorectal Tumor Surgery, First Affiliated Hospital of Xiamen University. We obtained written informed consent from all patients and approval from the hospital's ethical review board before using these clinical tissue specimens for research purposes.

2.4. Transfection

The shRNA for DPY30 plasmid and the control vector PLKO, the ovRNA for Raf1 plasmid and the control vector PLVX were bought from Public Protein/Plasmid Library (Geneppl, co, Ltd.). The generation of retrovirus supernatants, transfection for stable DPY30 knockdown cell lines HT29 and HCT116, then selected by puromycin for 7 days were prepared as described previously [26]. The pLVX-Puro-HA-Raf1 were transfected into cells using Lipofectamine® 3000 Reagent (Thermo Fisher Scientific, USA) in a 35-mm cell culture dishes following to the manufacturer's instructions.

2.5. Cell counting kit-8 assay

Human colorectal cancer cells were seeded into 96 well plate. After the adherent cell growth, cell proliferation was monitored by the Cell Counting Kit-8 (CCK-8) assay (Promega) according to the manufacturer's protocol. In addition, after the cells were treated with drugs for the corresponding time or transfected in advance, the preheated medium and CCK-8 were evenly mixed at a volume ratio of 10:1 to prepare a sufficient amount of CCK-8 reaction solution. The original medium was discarded, and 110 μL of CCK-8 reaction solution was added to each well and incubated at 37 °C for 3 h before spectrophotometry was performed at 450 nm.

2.6. Colony formation assay

Colorectal cancer cells HT29 and HCT116 (0.5×10^3 cells per well) were seeded in a six-well plate and incubated for 10–14 days after treatment. Then, the colonies were fixed with 4 % polyoxymethylene for 10 min at room temperature, washed three times with PBS, and stained with 0.5 % crystal violet for 5 min. The excess crystal violet was removed by washing three times with PBS. Then the number of colonies was counted using ImageJ.

2.7. Acridine orange/Ethidium bromide staining

AO and EB staining were used to visualize nuclear changes associated with apoptosis. AO is a vital dye that stains both live and dead cells, whereas EB stains only cells that have lost membrane integrity, indicating apoptosis. Live cells have normal nuclei staining that shows green chromatin with organized structures, while apoptotic cells have condensed or fragmented chromatin (bright green or orange red). Necrotic cells have similar normal nuclei staining as live cells except the chromatin is orange red instead of green [28]. After transfection, HT29 and HCT116 cells were incubated in 12-well plates for 48 h by starvation. Acridine orange/ethidium bromide (AO/EB) solution (5 μl; PBS solution of AO and EB 100 μg/ml) was added to each well for 5 min at room temperature. Cellular apoptosis was subsequently viewed and images were captured under a fluorescence microscope (Sangon, Shanghai).

2.8. Hoechst 33342 staining

An important feature of apoptotic cells is condensed or fragmented dense staining of nuclear chromatin. CRC cells at a density of 1×10^5 cells/well were cultured in six-well plates under 5 % CO_2 at 37 °C. The cells were treated with serum-free medium for 24 h. After the solution was removed and fixed with methanol for 10 min, it was washed three times with ice-cold PBS and stained with 1 μg/mL Hoechst 33342 at 37 °C for 15 min in the dark. This was followed by washing twice with PBS for 5 min each time. Antifade Mounting Medium with Hoechst 33342 was used to seal the slides, and finally the stained cells were visualized using a fluorescence microscope.

2.9. Western blotting

Cell and tissue protein lysates were separated by 10 % or 15 % sodium dodecyl sulfate-polyacrylamide gel electrophoresis (SDS-PAGE), transferred to 0.22-μm PVDF membranes (Millipore, Bedford, US) using eBlot protein transfer system (GenScript). The PVDF membrane was then blocked with 5 % skim milk for 3 h and incubated with specific antibodies overnight at 4 °C. Then incubated and conjugated with secondary antibodies for 1 h at room temperature before detection using an enhanced chemiluminescence reagent

Table 1
Primers designed for gene expression detection.

Application	Species	Gene	Forward primer (5′-3′)	Reverse primer (5′-3′)
expression	human	*DPY30*	AACGCAGGTTGCAGAAAATCCT	TCTGATCCAGGTAGGCACGAG
expression	human	*Raf1*	GGCAAACTCACAGATCCTTCTA	TCATGCAAGCTCATTCCATTTC
expression	human	*Bax*	GTCACTGAAGCGACTGATGT	CTTCTTCCAGATGGTGAGTGAG
expression	human	*Bad*	GACGAGTTTGTGGACTCCTTTA	CAAGTTCCGATCCCACCAG
expression	human	*Bak*	ACCCAGAGATGGTCACCTTA	GTCATAGCGTCGGTTGATGT
expression	human	*Bcl-2*	GTGGATGACTGAGTACCTGAAC	GAGACAGCCAGGAGAAATCAA
expression	human	*Bcl-xl*	GGTGGTTGACTTTCTCTCCTAC	TCTCCGATTCAGTCCCTTCT
ChIP	human	*Raf1-1*	TCGGCTCACCGCAATCTC	TGCCTGTCATCCCATCTACT
ChIP	human	*Raf1-2*	ACCGTTTAAGGTTCAGGGAC	ACAGGGCACAGTGTCCAA
ChIP	human	*Raf1-3*	GGCTGGAGTGTAATGGTGC	GGAGGCTGAGACAGGAGAAT
ChIP	human	*Raf1-4*	TCGCCTAACCTCTTCAGCT	TAACTTGGCTCGGGCATC
ChIP	human	*Raf1-5*	TACCTTGGACCAAACCGGATAT	TGGACAGTCCCTGAACCTTA

(Biothrive) and imaged using a Bio-Rad imaging system.

2.10. Hematoxylin and eosin (H&E) staining

The tumors isolated from the human, and the tissues were carefully kept in 10 % neutral formaldehyde for 24 h. After embedding in paraffin, the tissue blocks were sliced into 4-μm sections and mounted onto glass slides. The slices were dyed with hematoxylin solution for 5 min and then stained with eosin solution for 1 min. The color changes were observed under a microscope to control the degree of staining. After stained, those slices were slowly rinsed with distilled water for 10 min and dehydrated with gradient alcohol. After drying at room temperature and sealing with neutral resin, the morphological changes of the tissues were observed by optical microscopy.

2.11. Immunohistochemistry (IHC)

All specimens were fixed with 10 % neutral formaldehyde for 24 h and embedded in paraffin wax. The formalin-fixed paraffin-embedded tissue blocks were sliced into 4-μm sections and mounted onto glass slides. After dewaxing, the slides were first repaired with sodium citrate repair solution at high temperature for 5 min, followed by block with 3 % H_2O_2 peroxidase blocker buffer and 10 % donkey serum. Then, the slides were overnight incubated with specific primary antibody in a moist chamber at 4 °C. After washing thrice in phosphate-buffered saline (PBS), the slides were incubated with biotinylated goat anti-rabbit antibodies for 1 h. The slides were stained with DAB Kit (Maxim Biotechnologies) following the manufacturer's protocol. The slides were subjected by their counterstaining with Mayer's hematoxylin and dehydrated with gradient alcohol. The staining was observed under a microscope after sealing the slides with neutral resin.

2.12. Quantitative realtime reverse-transcription PCR (qRT-PCR)

Total RNA from cell lines was isolated using RNAsimple Total RNA kit (TIANGEN, DP419, China), and RNA were reverse transcribed into cDNA with FastQuant RT kit (with gDNase) (TIANGEN, KR106) following to the manufacturer's instructions. cDNA was generated using SuperReal PreMix Plus kit (TIANGEN, FP205) for qRT-PCR with ABI 7500 fast fluorescence temperature cycler. The primers used to detect human transcripts are listed in Table 1. The relative mRNA expression level of each gene was calculated by $2^{-\triangle\triangle Ct}$ method and compared with GAPDH. Each experiment was repeated three times.

2.13. RNA isolation and sequencing and transcriptome analysis

HT29 cells with stable knockdown of DPY30 were plated in 10-cm culture dishes for 48 h. After discarding the waste solution, the cells were rinsed three times with ice-cold PBS and total RNA was extracted using Trizol reagent kit. Following RNA quality assessed and enriched. The enriched mRNA was fragmented and reversly transcribed into cDNA. After end repaired and purified, cDNA library was sequenced using Illumina Novaseq 6000 by Gene Denovo Biotechnology Co. (Guangzhou, China). Differentially expressed genes (DEGs) were performed by DESeq2 software between six samples and performing the comparison between shCtrl and shDPY30. False discovery rate (FDR, adjusted *p*-value) ≤ 0.05 and fold change ≥ 1 were considered to filtrate genes. Then we screened for genes that were downregulated and upregulated in relation to apoptosis progression, following heatmaps were generated and designed via Omicsmart online platform. GO enrichment analysis was performed in the Gene Ontology database, gene numbers were counted for each GO term, significantly enriched GO terms in DEGs comparing to the genome background, which revealed the primary biological functions of DEGs.
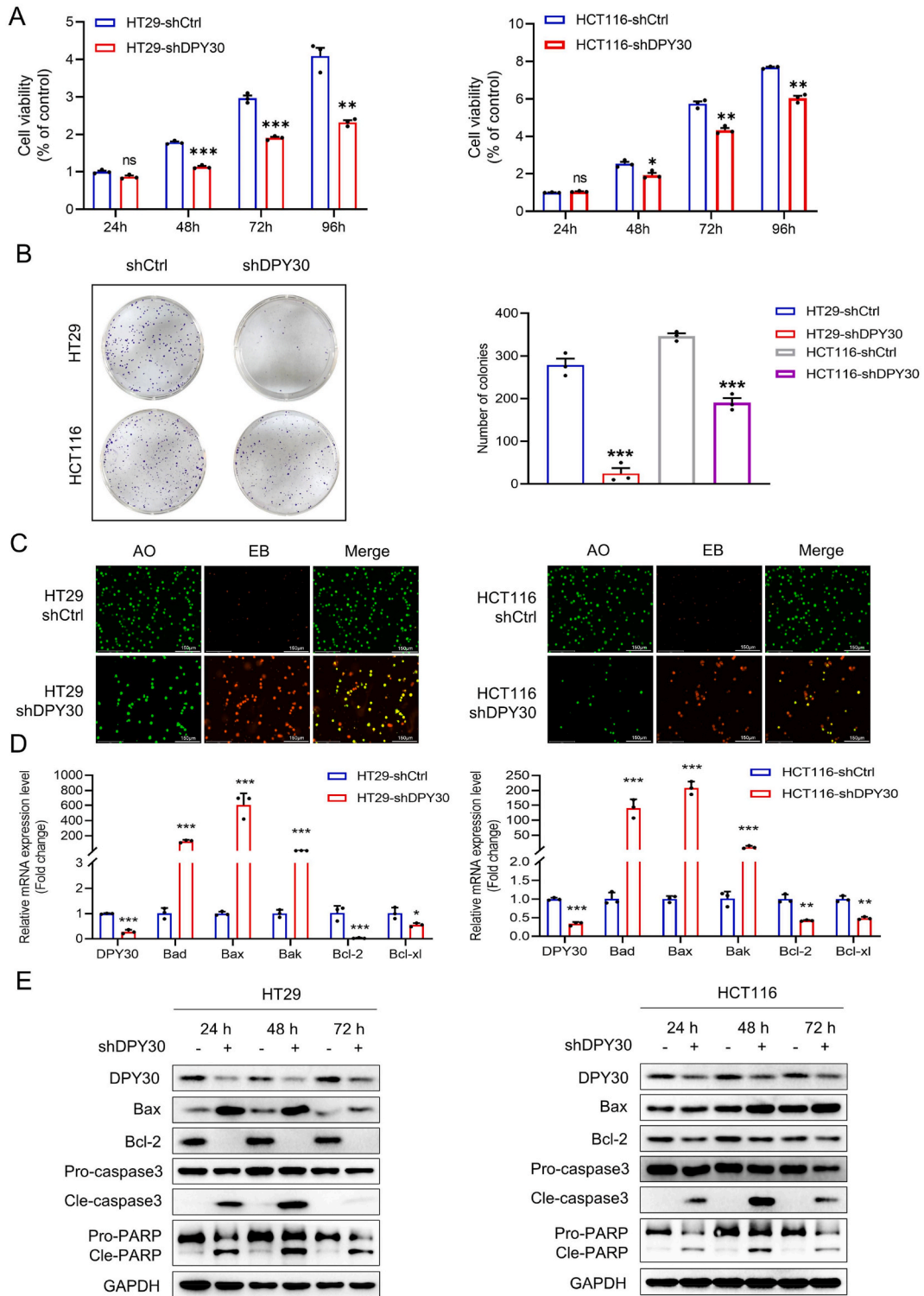
(caption on next page)

Fig. 1. The effect of DPY30 on cell proliferation and apoptosis of CRC cells. (A) Effects of DPY30 knockdown on the proliferation of CRC cells HT29 and HCT116 measured by CCK-8 assay. **(B)** DPY30 depletion weakened the colony formation ability of HT29 and HCT116 cell lines. The number of colonies is shown. **(C)** CRC cells were stained with acridine orange (AO) and ethidium bromide (EB) after transfection and viewed under a fluorescent microscope. In this case, nonapoptotic cells are shown in green, and cells undergoing apoptosis are bright green and red in the nucleus (Scale bar:150 µm). **(D)** DPY30 suppression using specific shRNA resulted in a significant up-regulation of the pro-apoptotic genes, including Bad, Bak, and Bax. Additionally, DPY30 knockdown caused a remarkable down-regulation in the expression of anti-apoptotic genes, Bcl-2 and Bcl-xl. **(E)** DPY30 knockdown increased the proteins expression levels of Cleaved-PARP, Cleaved-caspase 3 and Bax and weakened the proteins expression level of Bcl-2 in HT29 and HCT116 cells. Data were expressed as mean ± SEM. NS, no significant difference, *P < 0.05, **P < 0.01, ***P < 0.001.

2.14. Apoptosis detection

Apoptosis ratio is often detected by flow cytometry (FCM). CRC cells were cultured in six-well plates under 5 % CO_2 at 37 °C. After adherent, cells were starved in serum-free medium or treated with CCCP (20 µM) and Z-VAD-FMK (10 µM) for 24 h. Then, cells were gently washed with ice-cold phosphate-buffered saline (PBS) three times, digested and collected into 5 ml tubes. Next, the cells were resuspended in 400 µl binding buffer (BD Biosciences, CA, USA), stained with 5 µl Annexin-V-FTIC (BD Biosciences, CA, USA) and 5 µl propidium iodide (BD Biosciences, CA, USA), and incubated at room temperature in the dark for 20 min. All apoptosis rates were measured by FCM within 1 h. Their percentages were discriminated from a bivariate histogram of only Annexin-V-FTIC-labeled cells.

2.15. Chromatin immunoprecipitation assay (ChIP)

In order to conduct the ChIP assay, we used the SimpleChIP® Plus Sonication Chromatin IP Kit (Cell Signaling Technology, USA). Briefly, a 15-min cross-linking procedure was performed on HT29 and HCT116 cells using 1 % formaldehyde in 10-cm culture dishes. A glycine solution was used to quench cells before they were washed and scraped to obtain cell pellets. After lysing and fragmenting the cell via Bioruptor sonication, the chromatin was incubated overnight at 4 °C with anti-H3K4me3 antibody or anti-rabbit IgG antibody. ChIP-Grade Protein G Magnetic Beads were then used to precipitate the complexes for another 2 h at 4 °C. After washes, chromatin from Antibody/Protein G Magnetic Beads was eluted. After capturing the protein-DNA, it was de-crosslinked with 5 M NaCl and Proteinase K for 2 h at 65 °C. Finally, it was purified using spin columns as instructed by the manufacturer and amplified by qPCR with primer pairs (Table 1). Antibodies were also purchased from Cell Signaling Technology and used at recommended concentrations.

2.16. Statistical analysis

The results were analyzed using GraphPad Prism version 8.0.1 and represented as the mean ± SEM of at least three biological replicates. Two-tailed Student's t-tests and ANOVA were used to analyze the data. Pearson correlation was used to test the association between Raf1 expression and DPY30 expression. The difference was considered to be statistically significant at *P < 0.05, **P < 0.01, ***P < 0.001.

3. Results

3.1. DPY30 knockdown suppressed proliferation and induced apoptosis in CRC cells

To evaluate the biological role of DPY30 in colorectal cancer cell growth, The typical CRC cell lines HT29 and HCT116 cells, from which DPY30 is relatively abundant expressed, were used for subsequent studies. The cell viability results indicated that DPY30 knockdown significantly inhibited the growth of CRC cells by CCK-8 assay (Fig. 1A), and inhibited colony formation ability obviously by colony formation assays (Fig. 1B). Moreover, acridine orange/ethidium bromide (AO/EB) staining indicated that DPY30 knockdown was followed by an elevated number of apoptotic cells in HT29 and HCT116, compared to shCtrl-transfected cells (Fig. 1C). This indicated that DPY30 knockdown induced apoptosis in CRC cells. Then we found that the relative levels of pro-apoptotic genes were significantly up-regulated (*Bad, Bak, Bax*), while the relative levels of anti-apoptotic genes were significantly decreased (*Bcl-2, Bcl-xl*) in CRC cells when DPY30 knockdown by qRT-PCR (Fig. 1D). Additionally, Western blot assay was performed to determine whether DPY30 knockdown induces apoptosis (Fig. 1E, Supplement File 1). The results showed that the relative levels of pro-apoptotic protein Bax increased, while the anti-apoptotic protein Bcl-2 decreased dramatically at 24 h, 48 h and 72 h. In addition, loss of DPY30 resulted in cleavage of caspase-3 and PARP, which induced HT29 and HCT116 cells apoptosis. According to these results, DPY30 is an important regulator of CRC cell survival, and knockdown induces apoptosis.

3.2. DPY30 knockdown induced apoptosis of CRC cells through caspase activation

To further clarify that DPY30 knockdown induced apoptosis in CRC cells, the apoptosis inducer CCCP and apoptosis inhibitor Z-VAD-FMK were used respectively to detect their effects on the changes of DPY30 knockdown induced apoptosis. Then, we assessed the effects of DPY30 depletion on HT29 and HCT116 cells by staining with Hoechst 33342 and observing their fluorescence under a microscope. Treatment of DPY30 knockdown cells with cell apoptosis inducer CCCP for 24 h led to an increase in nuclear condensation and fragmentation, but cell apoptosis inhibitor Z-VAD-FMK reverses this phenomenon (Fig. 2A). Then we evaluated CCCP and Z-VAD-FMK on cell viability and apoptosis ratio of DPY30-knockdown cells by treating with them a serum-free medium. The percentage of cell
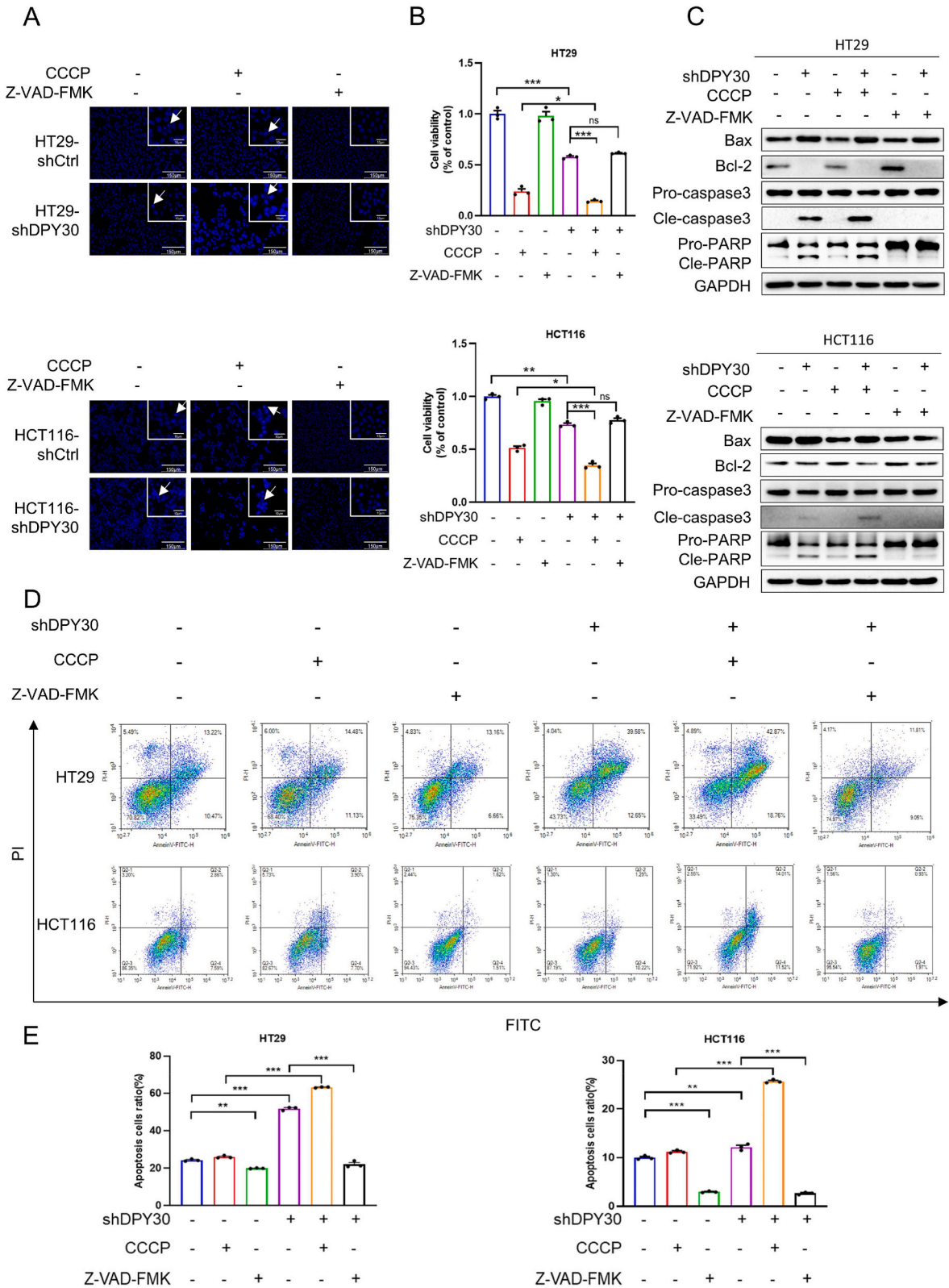
(caption on next page)

Fig. 2. CCCP and Z-VAD-FMK regulates the apoptosis of CRC cells induced by DPY30 depletion. (A) Hoechst 33342 staining was used to evaluate apoptotic morphology by fluorescence microscopy. Highly condensed or fragmented nuclei represent apoptotic cells (Scale bar:150 μm). **(B)** Effect of DPY30 knockdown on cell viability of HT29 and HCT116 cells in the presence or absence of CCCP (20 μM) or Z-VAD-FMK (10 μM) for 24 h by CCK-8 assay. **(C)** Effect of DPY30 knockdown on the expression of pro-apoptotic and anti-apoptotic proteins in the presence or absence of CCCP (20 μM) or Z-VAD-FMK (10 μM) for 24 h by western blotting. **(D)** The representative images of cell apoptosis in HT29 and HCT116 cells after DPY30 knockdown with the treatment of CCCP (20 μM) or Z-VAD-FMK (10 μM). **(E)** The statistical results of cell apoptosis in HT29 and HCT116 cells after DPY30 knockdown with the treatment of CCCP (20 μM) or Z-VAD-FMK (10 μM) for 24 h. Data were expressed as mean ± SEM. NS, no significant difference, *$P < 0.05$, **$P < 0.01$, ***$P < 0.001$.

viability affected by CCCP was significantly decreased when DPY30 knockdown, while Z-VAD-FMK inhibited the decrease in cell viability mediated by DPY30 knockdown (Fig. 2B). Furthermore, Western blot analysis also carried out that CCCP increased protein expression levels of Bax, Cleaved PARP, Cleaved caspase-3, and decreased Bcl-2 in DPY30-deficient CRC cells, while Z-VAD-FMK reversed this phenomenon (Fig. 2C, Supplement File 1). And the apoptosis ratio, detected with flow cytometry via Annexin-V-FTIC staining, its apoptosis level was significantly increased after DPY30 downregulation. In addition, CCCP significantly promoted apoptosis after DPY30 downregulation, and Z-VAD-FMK significantly inhibited apoptosis after DPY30 downregulation (Fig. 2D and E). Taken together, these results showed that CCCP increased the apoptosis of CRC cells induced by DPY30 knockdown, while Z-VAD-FMK inhibited the apoptosis of CRC cells induced by DPY30 knockdown.

3.3. DPY30 knockdown modulated the biological processes of apoptosis and apoptosis-related gene Raf1 based on RNA-seq

Given that DPY30 is involved in the activation of gene expression, we performed RNA sequencing analysis and focused on possible regulators critical for CRC cells apoptosis. Through the GO analysis of biological processes, in the process of cell death, the differential genes were mainly enriched in the process of apoptosis after DPY30 knockdown. For example, cell death, programmed cell death and apoptotic process, *etc*. (Fig. 3A). The heat map revealed significant differential expression of apoptosis-related genes, including Bcl2, AKT3, NFκB1, PARP1, and Raf1, *etc*. Notably, Raf1 transcription level was significantly down-regulated after DPY30 knockdown, is highlighted in red with a box. (Fig. 3B). In addition, KEGG pathway enrichment analysis showed that the differentially expressed genes were most closely related to the Hippo pathway (Fig. 3C). O'Neill et al. [29] showed that Raf1 interferes with the dimerization and phosphorylation of MST2 by directly binding to MST2. As a result, MST2-mediated apoptosis was prevented. Therefore, we speculate that DPY30 may affect the Hippo signaling pathway through Raf1 to mediate the apoptosis of CRC cells. We found that DPY30 knockdown decreased Raf1 mRNA and protein expression levels, and increased p-MST2 and p-YAP protein levels in the Hippo pathway (Fig. 3D and E, Supplement File 1). RNA-seq, qRT-PCR and WB quantification results showed that Raf1 expression level was substantially correlated with DPY30's expression level (Fig. 3F). According to the above results, DPY30 may regulate CRC cells apoptosis through Raf1 and Hippo pathways.

3.4. Knockdown of DPY30 promoted apoptosis of CRC cells by suppressing Raf1 expression

To determine whether Raf1 mediates the protective effect against knockdown DPY30-induced apoptosis in CRC cells. DPY30 knockdown CRC cells were transfected with Raf1-overexpression plasmid to promote its expression for 48 h with Hoechst 33342 and observed nuclear condensation and fragmentation increased (Fig. 4A). Furthermore, Raf1 overexpressed in DPY30 knockdown CRC cells resulted in cell viability increasing significantly (Fig. 4B) and apoptotic cells decreased compared to the control cells (Fig. 4C). Similarly, Western blot results confirmed that Raf1 overexpression inhibited apoptosis mediated by DPY30 knockdown (Fig. 4D, Supplement File 1). These results indicated that Raf1 overexpression inhibited the apoptotic phenotype of DPY30 down-regulated CRC cells *in vitro*.

3.5. DPY30 regulated CRC cells apoptosis via Raf1-MST2 signaling axis

DPY30 is a part of the key components of the mammalian SET1/MLL histone methyltransferase complex. Previous reports have shown that DPY30 regulates three different forms of H3K4 methylation levels on genes, particularly the function of H3K4me3 [16]. Therefore, we treated CRC cells with histone methyltransferase inhibitor MM102 for 48 h, and found that Raf1 protein and gene expression levels were significantly reduced compared with the control group by WB and qRT-PCR (Fig. 5A, Supplement File 1). We then explored whether DPY30 expression was associated with H3K4me3 modification at the Raf1 promoter. Five pairs of primers for the Raf1 gene promoter region were designed (Fig. 5B). As shown by ChIP-qPCR, less occupancy of those raf1 gene promoter regions by H3K4me3 when DPY30 knockdown (Fig. 5C). DPY30 knockdown attenuated H3K4me3 levels at region −471 to −365 bp (P2, *$P < 0.05$*), −1134 to −1055 bp (P3, *$P < 0.01$*), −217 to −111 bp (P4, *$P < 0.05$*) and −564 to −446 bp (P5, *$P < 0.001$*) of the Raf1 gene promoter in HT29-shDPY30 cells, and region −217 to −111 bp (P4, *$P < 0.05$*) and −564 to −446 bp (P5, *$P < 0.001$*) in HCT116-shDPY30 cells. In addition, DPY30-knockdown CRC cells were transfected with a certain amount of Raf1 overexpression plasmid. At 48 h after transfection, Western blot confirmed that overexpression of Raf1 reduced the increase of p-MST2 and p-YAP protein expression levels caused by DPY30 deletion to a certain extent (Fig. 5D, Supplement File 1). These results demonstrated that DPY30 knockdown induced Raf1 transcriptional inactivation by regulating H3K4me3, and confirmed that the regulation of apoptosis by DPY30 and Raf1 was partly dependent on MST2.

A

| GO analysis of transcripts detected as up-regulated upon DPY30 knockdown			
Gene ontology of biological process	Gene percent (%)	Raw p-value	Q-value(FDR)
cell death (GO:0008219)	14.64%	1.40E-07	8.90E-06
programmed cell death (GO:0012501)	13.73%	2.44E-07	1.42E-05
apoptotic process (GO:0006915)	12.97%	5.20E-08	3.51E-06
regulation of cell death (GO:0010941)	11.75%	5.77E-10	5.48E-08
regulation of apoptotic process (GO:0042981)	10.69%	2.14E-09	1.90E-07
positive regulation of cell death (GO:0010942)	5.48%	5.11E-10	4.97E-08
apoptotic signaling pathway (GO:0097190)	4.15%	3.29E-04	7.11E-03
programmed necrotic cell death (GO:0097300)	0.47%	2.09E-03	3.00E-02

B

C

D

E

F
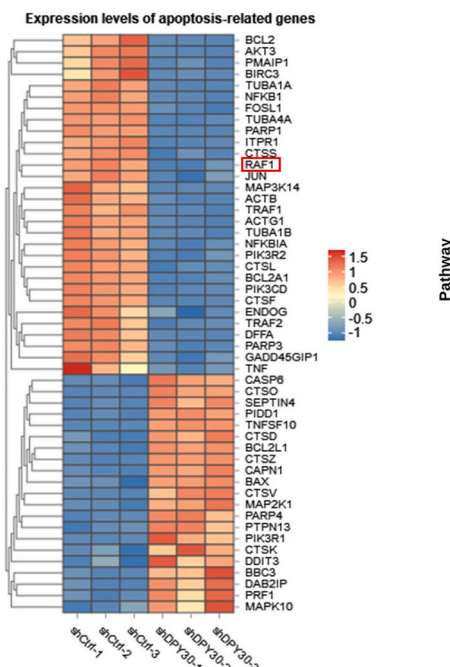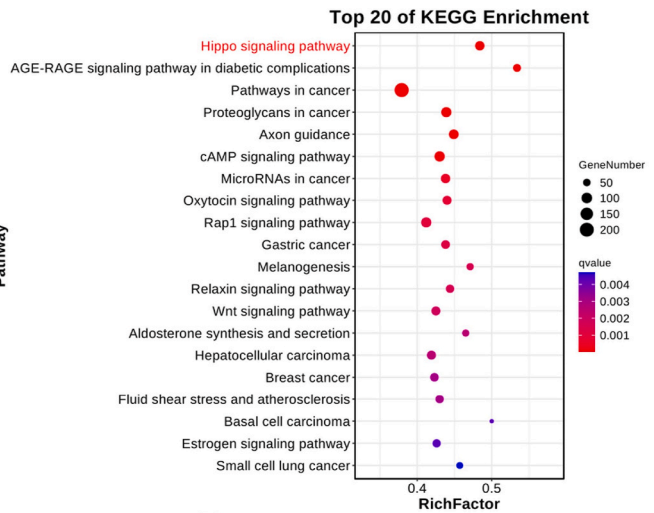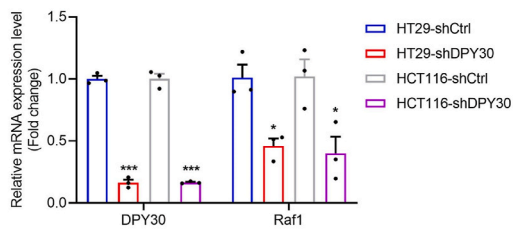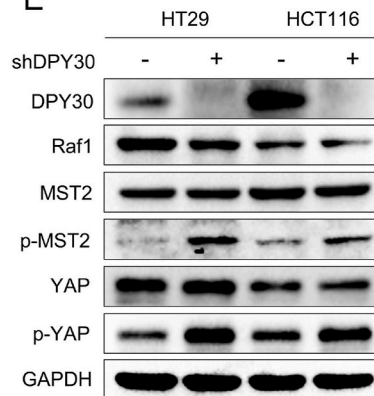
	RNA-Seq		qRT-PCR		WB	
Gene Symbol	Ratio	Adjusted p(ANOVE)	Ratio	p(ANOVE)	Ratio	p(ANOVE)
Raf1	-2.046577096	1.80E-35	-2.1773068	0.0106	-1.731727446	<0.0001
DPY30	-2.015905676	1.17E-27	-6.10810117	<0.0001	-8.243414574	<0.0001

(caption on next page)

Fig. 3. To screen the downstream effector Raf1 of DPY30 based on RNA-seq and confirms that DPY30 regulates apoptosis of colorectal cancer cells through Hippo signaling pathway. (A) Gene ontology (GO) analysis for genes up-regulated by DPY30 knockdown in HT29 cells (FDR <0.05 and fold change ≥1). **(B)** Heatmaps representing unsupervised hierarchical clustering of mRNA expression level depicting down-regulated and up-regulated genes of FDR <0.05 associated with apoptotic progression. Each column represents the indicated sample. **(C)** Bulb map for KEGG enrichment analysis of genes altered by DPY30 in HT29 cells. The Hippo signaling pathway is highlighted in red. Rich factor represented the enrichment degree of differentially expressed genes. Y axis showed the name of enriched pathways. The area of each node represented the number of the enriched host genes of differentially expressed RNAs. The q-value was represented by a color scale. The statistical significance increased from blue (relatively lower significance) to red (relatively higher significance). **(D)** DPY30 knockdown caused a remarkable down-regulation in the expression of Raf1 genes. **(E)** Depletion of DPY30 promoted expression of Raf1 and Hippo signaling pathway - related protein, including p-MST2, p-YAP. **(F)** Mean gene or protein expression levels were set to one in HT29-shCtrl cells for RNA-Seq, qRT-PCR and western blotting data. Gene or protein expression ratios by RNA-Seq, qRT-PCR and western blotting data are shown as is the *p value* (one-way ANOVA). Data were expressed as mean ± SEM, **P < 0.05, **P < 0.01, ***P < 0.001.*

3.6. The expression of DPY30 is positively correlated with Raf1-MST2 in CRC

To further explore the relationship between DPY30/Raf1/p-MST2 signaling pathway in the clinical context, we evaluated their expression levels in surgical specimens. Then, endogenous protein expression levels of DPY30, Raf1 and p-MST2 were analyzed in a series of paired human colorectal carcinomas (T) and autologous adjacent normal tissues (N) by western blotting (n = 25) (Fig. 6A, Supplement File 1). In tumor specimens, the high expression rates of DPY30 and Raf1 were 80 % and 84 %, respectively, and the low expression rate of p-MST2 was 68 %. In tumor specimens, a median relative expression of 2.8-fold for DPY30, 1.5-fold for Raf1 and 0.6-fold for p-MST2 compared with normal tissue were derived, indicating that both DPY30 and Raf1 were highly expressed and p-MST2 was low expressed in tumors (Fig. 6B). Next, we observed the structure and histomorphology of subcutaneously transplanted tumors in nude mice (Fig. 6C) and human CRC tissues (Fig. 6D) by H&E staining. And we found that adjacent normal tissues and DPY30 knockdown nude mice tissues exhibited relatively low expression of DPY30 and Raf1, in contrast, colorectal cancer tissues and tissues from nude mice compared with knockdown control had high DPY30 and Raf1 expression by IHC (Fig. 6C and D). Moreover, the correlations between the expression levels of DPY30 and apoptosis-related genes in CRC were further analyzed by GEPIA2 database (http://gepia2.cancer-pku.cn/, COAD and READ in TCGA expression data) (Fig. 6E), the results showed that the expression of DPY30 was positively correlated with Bcl-2 and Raf1, and negatively correlated with Bax, which were in concordance with data obtained in our experiment. DPY30 is positively correlated with the Raf1/p-MST2 axis in CRC.

4. Discussion

Colorectal cancer is one of the most common digestive system tumors worldwide, and its rapid disease progression and advanced tumor presentation are associated with a high mortality rate [2,30]. There is an urgent need to find potential targets and new treatment strategies for CRC. In previous studies, epigenetic modifications have been found to be crucial to the diagnosis and treatment of CRC [31,32]. As a core subunit of histone methyltransferase, DPY30 plays an important role in epigenetic modification affecting tumor development [10]. DPY30 has been reported in gastric cancer, ovarian cancer, and cholangiocarcinoma, showing up-regulated expression and cancer-promoting characteristics in these epithelial tumors, and is associated with poor prognosis of tumor patients. The difference is that the mechanism of DPY30 promoting cancer progression is different. Reports show that DPY30 can regulate cell proliferation and differentiation by affecting the expression of MYC oncoprotein and ID protein and the transcriptional activity of E2F. It has been found that the expression level of DPY30 can affect the EMT process in cervical squamous cell carcinoma [25]. Jeremy N. Rich reported that DPY30 regulated the expression of PDE4B in glioblastoma depending on H3K4me3, thus regulating angiogenesis and hypoxia pathways [33]. Moreover, the role of DPY30 in the death progression of CRC cells has not been characterized. Therefore, the correlation between DPY30 and tumor cell apoptosis and its downstream positive regulatory mechanism deserves further in-depth study. The purpose of this question was to determine the correlation between altered DPY30 expression and apoptosis and whether it could be used as a new target for CRC treatment. This question will help to more comprehensively analyze the biological function of DPY30, and provide new insights and ideas for the application of DPY30 in the early diagnosis and treatment of CRC in the future.

In this study, we investigated DPY30's functional significance and possible utility as a therapeutic target or biomarker in CRC. We demonstrated that the protein level of DPY30 was highly expressed in CRC tissues. We then used lentivirus-mediated shRNA to silence DPY30 expression in CRC cells. CCK-8 assay showed that the knockdown of DPY30 significantly reduced cell proliferation in HT29 and HCT116 cells. Western Blot was used to detect the expression of apoptosis-related proteins in DPY30 knockdown cells and control cells at different time points of starvation, and it was found that the expression of apoptosis-related proteins was more obvious after 48 h of starvation, which may be because it takes a certain time for DPY30 knockdown to induce apoptosis in cells. What's more, DPY30 downregulation leads to altered expression of a series of genes, which in turn causes the onset of apoptosis, which requires a process. Flow cytometry was used to determine the promoting effect of DPY30 depletion on apoptosis in HT29 and HCT116 cells. It was confirmed that DPY30 knockdown induced cell death was the way of apoptosis by the positive and negative complement of apoptosis specific inducer and inhibitor. These results suggest that DPY30 may play a key role in promoting CRC cell proliferation and inhibiting apoptosis and play an oncogenic role in the development of CRC.

Cell apoptosis can be induced by intrinsic and extrinsic pathways. The intrinsic pathway is the most prevalent way, which can be activated by intracellular signals when cells are stimulated, such as with the caspase signaling pathway [34]. Meanwhile, in the intrinsic pathway of apoptosis, Members of the Bcl family including Bax and Bcl-2, known as pro- or antiapoptotic proteins
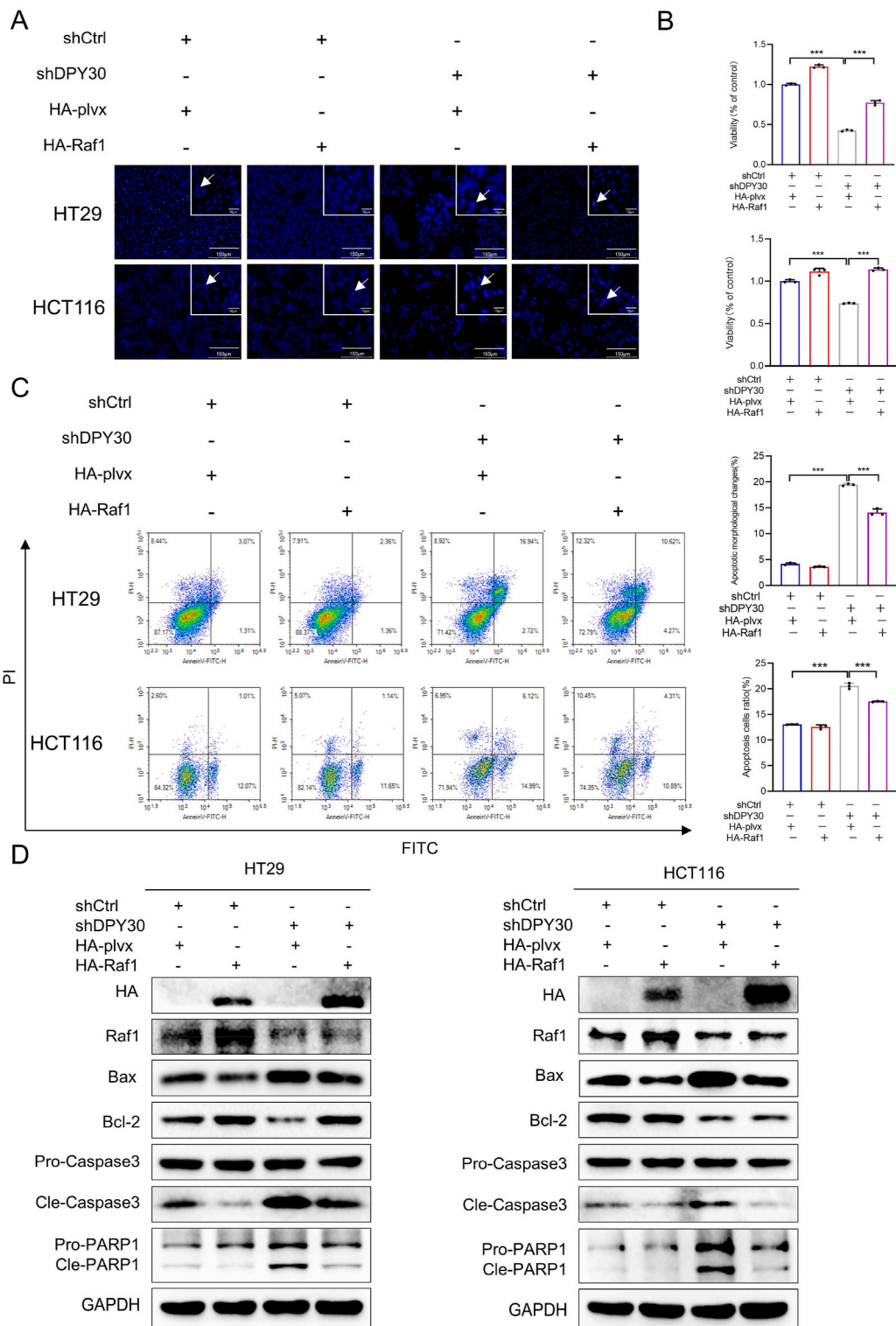
Fig. 4. Knockdown of DPY30 promoted apoptosis of colorectal cancer cells by affecting Raf1. (A) Representative phase-contrast images of HT29 and HCT116 cells showed Raf1 overexpression rescued colorectal cancer cell apoptosis induced by DPY30 knockdown. Hoechst 33342 staining was used to evaluate apoptotic morphology by fluorescence microscopy. Highly condensed or fragmented nuclei represent apoptotic cells. (Scale bar:150 μm). **(B)** CCK-8 assay detected the inhibitory effect of Raf1 overexpression on DPY30 knockdown induced apoptosis in colorectal cancer cells. **(C)** HT29 and HCT116 cells stably knocked-down DPY30 were transiently transfected with HA-Raf1 expression plasmid. Apoptosis was determined assessing DNA fragmentation by flow cytometry two days post-transfection. The representative images of cell apoptosis (left). The statistical results of cell

apoptosis (right). **(D)** Raf1 overexpression partly counteracts DPY30 knockdown induced apoptosis. DPY30 knockdown HT29 and HCT116 cells were transfected with indicated amounts of a Raf1 expression plasmid. After 48 h post transfection, cells were lysed, and Raf1, HA, pro-apoptotic and anti-apoptotic proteins expression levels were assessed by western blotting. Data were represented as mean ± SEM from three independent experiments at least. *$P < 0.05$, **$P < 0.01$, ***$P < 0.001$.

respectively, present on the mitochondrial membrane, are the key mediators for the intrinsic apoptotic pathway [35]. In addition, they are activated and bind to the mitochondrial outer membrane, forming a hole in the membrane through which some proteins in the mitochondria can enter the cytoplasm and eventually form apoptotic bodies. These apoptotic bodies had the effect of cleaving the effector apoptotic protease caspase-3, which is activated by cleavage and then causes the degradation of downstream proteins related to cell life, and finally causes cell apoptosis. Importantly, previous reports suggesting that higher levels of apoptosis in tumors may lead to a better prognosis may be logical. Apoptosis mediated by intrinsic or extrinsic pathways leads to the cleavage of Caspase-3 and Caspase-7. Caspase-3 is rarely mutated in CRC and is therefore an ideal marker for assessing apoptosis in these tumor cells [36]. Our results confirmed that CRC cells lacking DPY30 had significantly higher levels of cleaved Caspase-3. As an additional confirmation of apoptosis, caspase-3-mediated cleavage of poly (ADP-ribose) polymerase (PARP) was measured in CRC cells. DPY30 knockdown increased the activation of these two apoptosis-related molecules, which strongly confirms that the effect of DPY30 on CRC cell apoptosis *in vitro* is an endogenous pathway dependent on caspase activation. This process is part of the apoptotic pathway, and although some studies have been conducted, the specific apoptotic signal transduction mechanism needs to be further improved.

Therefore, in order to elucidate the molecular mechanism of DPY30 affecting the apoptosis of CRC cells, transcriptomic sequencing analysis revealed that DPY30 knockdown affected the modification of some apoptosis-related molecules and the Hippo signaling pathway. Previous studies suggest that the constitutive activation of the PI3K/AKT pathway contributes to epigenetic alterations in tumor progression [37,38]. PI3K stimulates the signaling cascade and promotes the activation of AKT, an important regulator of cell growth signaling. AKT plays an anti-apoptotic role in several varieties of cell death, as well as the disruption of extracellular signaling molecules, oxidation, osmotic stress, and ischemic shock [39]. Gong Cheng et al. have shown that DPY30 knockdown suppressed the activation of the PI3K/AKT signaling pathway in OS cells, which underlies the functional role of DPY30 [40]. NF-κB is the downstream effectors of the PI3K/Akt/mTOR pathway [41]. Meiling Yu reported that PI3K/Akt/NF-κB pathway could control CDDP resistance via EMT and NF-κB-mediated apoptosis, and the Baicalein compound significantly suppress the PI3K/Akt/NF-κB pathway [42]. And PI3K/AKT/NF-κB/BMP-2-Smad axis signaling could regulate tumor cell metastasis and invasion [43]. NF-κB is also a transcription factor that plays an important biological function in many cells, including immune response, cell proliferation and apoptosis. As for their association with epigenetics, it has been reported that apoptosis of neoplastic cells is prevented by alterations of NF-κB and the PI3K/AKT/mTOR axis. virus infection can simultaneously activate JAK/STAT and NF-κB, leading to evasion of apoptosis, effecting epigenetic phenomena such as promoter hypermethylation, which leads to the downregulation of tumor-suppressor regulation genes [44].

Here, we plan to explore a completely new signaling pathway. The Hippo pathway is an evolutionarily and functionally conserved regulator of organ size and growth with crucial roles in cell proliferation, apoptosis, and differentiation [45]. In this pathway, MST1/2 has been regarded as the focus of research, because MST1/2 participates in the regulation of apoptosis under external stimuli [46]. MST1/2 are activated by autophosphorylation and caspase-dependent cleavage [47–49], which liberates the ~35 kDa N-terminal kinase domain from a C-terminal autoinhibitory domain; active kinase then translocates the nucleus and promotes apoptosis by phosphorylating relevant substrates such as Histone H2B [50]. Furthermore, Raf-1 was screened and confirmed as a potential DPY30-important effector. Based on previous studies, the anti-apoptotic effect of Raf1 has been reported by preventing the dimerization of p-MST2 and reducing the kinase activity of MST2, leading to the reduction of apoptosis [29]. Our study found that the protein and gene levels of Raf1 were significantly down-regulated after DPY30 knockdown, and the protein level of p-MST2 was significantly increased. Importantly, transient overexpression of Raf1 restored the apoptosis induced by DPY30 knockdown in CRC cells. What's more, the addition of MM102, a histone methyltransferase inhibitor, resulted in reduced histone methylation levels, which in turn resulted in reduced gene and protein expression levels of Raf1. Mechanistically, the knockdown of DPY30 inhibited the establishment of H3K4me3 in the Raf1 promoter region, resulting in decreased transcription levels. Therefore, we found and clarified that DPY30 inhibits CRC cells apoptosis by positively regulating Raf1/MST2 axis. However, in this study, the relationship between Raf1 and MST2 has not been studied and confirmed in CRC. The more specific mechanism of DPY30 inhibiting CRC cells apoptosis by regulating the Raf1/MST2 axis in colorectal cancer and the upstream and downstream signal transduction mechanism will be further studied in the future.

5. Conclusion

In conclusion, it was found that DPY30 downregulation promotes MST2-induced apoptosis by inhibiting Raf1 transcriptional activity through histone H3 lysine 4 trimethylation (H3K4me3) *in vitro*, and a strong correlation was also observed at the clinical sample level. These studies provide novel insights into the function of DPY30 in CRC cells that were previously unknown. A better understanding of the downstream target genes and pathways affected by epigenetic influences regulated by DPY30 will facilitate the development of novel small molecule inhibitors with selective apoptosis-inducing effects on CRC (Fig. 7, **Graphical Abstract**). As a result of our research, we have provided a new theoretical and experimental basis for the pathogenesis of CRC, and inhibition of the DPY30/Raf1/MST2 axis may provide a new strategy for the treatment of CRC.
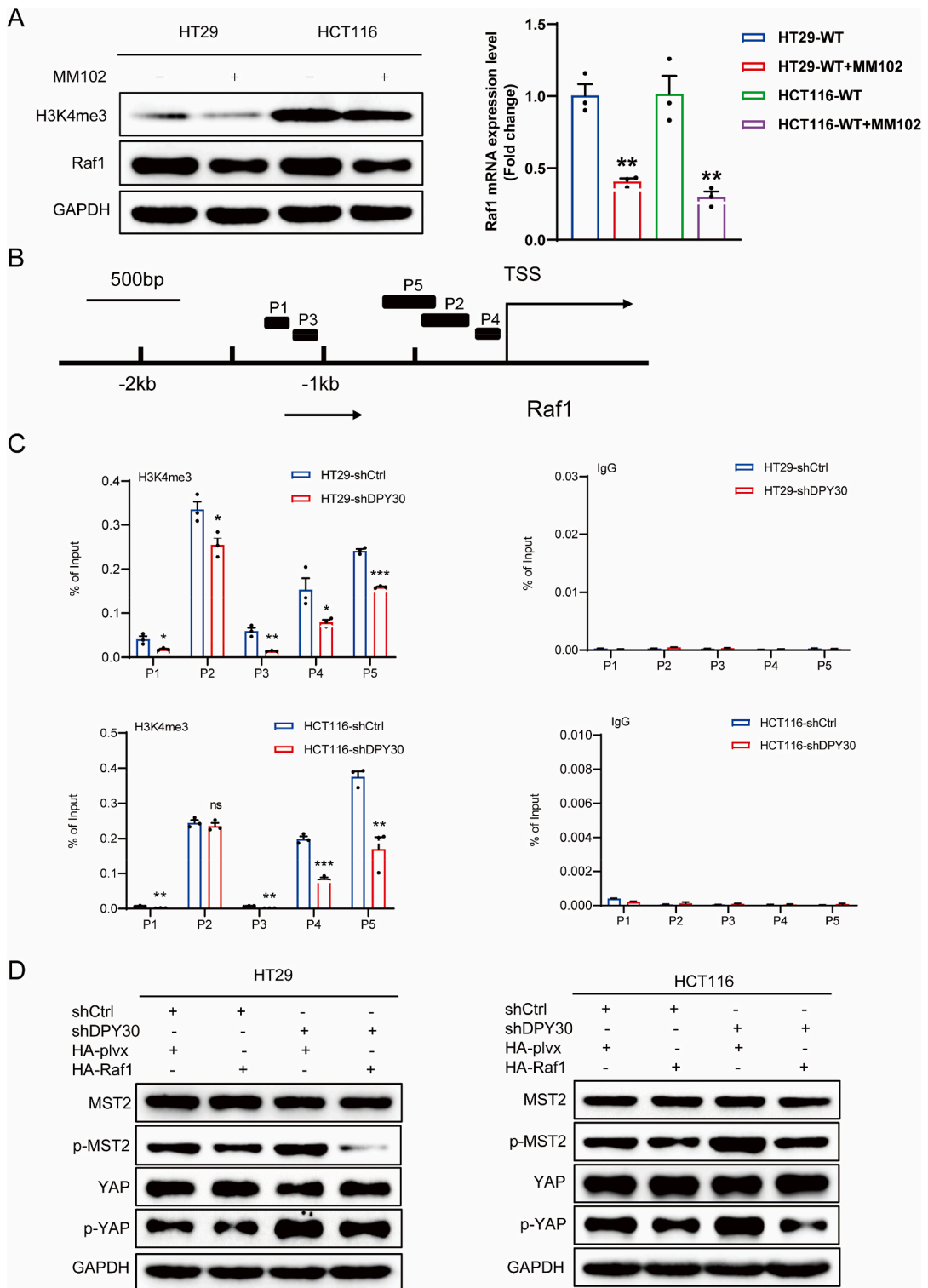
Fig. 5. DPY30 mediates CRC cell apoptosis by regulating Raf1-MST2 signaling axis. (A) The effect of histone methyltransferase inhibitor MM102 (20 μM) on the expression level of Raf1 and H3K4me3 in colorectal cancer cells treated with for 48 h was detected by WB (left) and qRT-PCR (right). **(B)** Schematic presentation of the five regions relative to the Raf1 transcriptional start site used as primers to test H3K4me3 occupied abundance. **(C)** ChIP-qPCR was performed to assess H3K4me3 occupancy to Raf1 transcriptional start site in HT29-shDPY30, HCT116-shDPY30 and their control cells (left). IgG was used as negative control (right). "Percentage of input" indicates the ratio of DNA fragment of each promoter region bound by H3K4me3 to the total amount of input DNA fragment without H3K4me3 antibody pull-down. **(D)** Raf1 overexpression partly counteracts DPY30 knockdown induced apoptosis. DPY30 knockdown HT29 and HCT116 cells were transfected with indicated amounts of a Raf1 expression plasmid. After 48 h post transfection, cells were lysed, and p-MST2 and p-YAP proteins expression levels were assessed by western blotting. Data were represented as mean ± SEM from three independent experiments at least. *P < 0.05, **P < 0.01, ***P < 0.001.
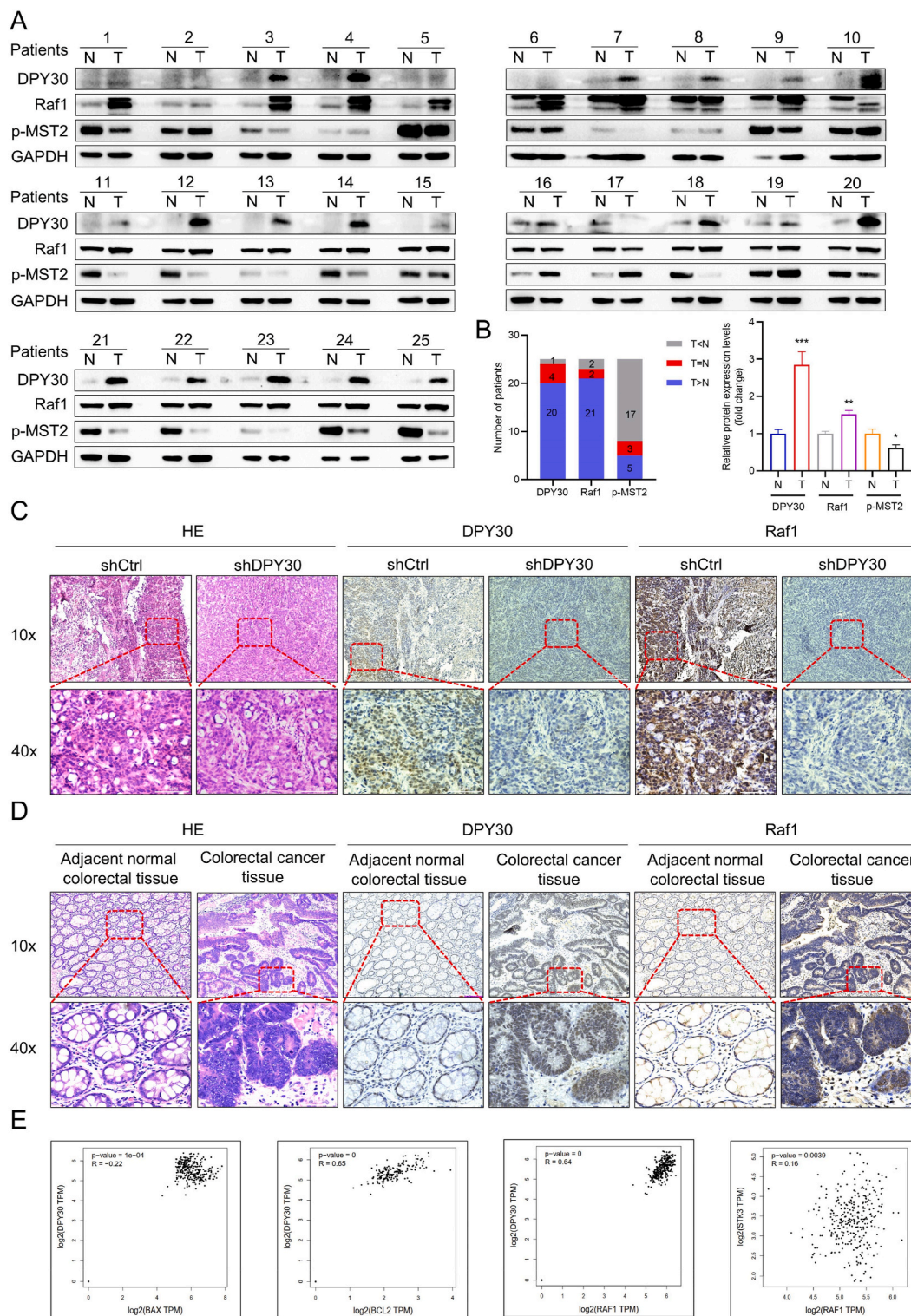
Fig. 6. The correlation between DPY30/Raf1/MST2 in online database, clinical CRC tissues and nude mouse subcutaneous tissues. (A) The correlation between DPY30, Raf1 and p-MST2 proteins expression levels were detected by WB in 25 cases of human colorectal cancer tissues. **(B)** The number of patients with high expression of DPY30 and Raf1 and low expression of p-MST2 in tumors were respectively counted in the bar chart (left). Relative expression of DPY30, Raf1 and p-MST2 proteins according to disease state of the tissue (right). **(C)** Representative hematoxylin-eosin and immunohistochemical staining of tissue sections from shCtrl and shDPY30 nude mouse subcutaneous tumors (10 ×, Scale bar:275 µm; 40 ×, Scale bar:75 µm). **(D)** Representative hematoxylin-eosin and immunohistochemical staining of DPY30, and Raf1 protein expression in colorectal

cancer tissue specimens (10 ×, Scale bar:275 μm; 40 ×, Scale bar:75 μm). **(E)** The correlations between DPY30 with Bax, Bcl2 and Raf1, Raf1 with MST2 were evaluated in the GEPIA database. R, correlation coefficient. Positive number indicated positive correlation and negative number indicated negative correlation. Data were represented as mean ± SEM from three independent experiments at least. *$*P < 0.05, **P < 0.01, ***P < 0.001$*.
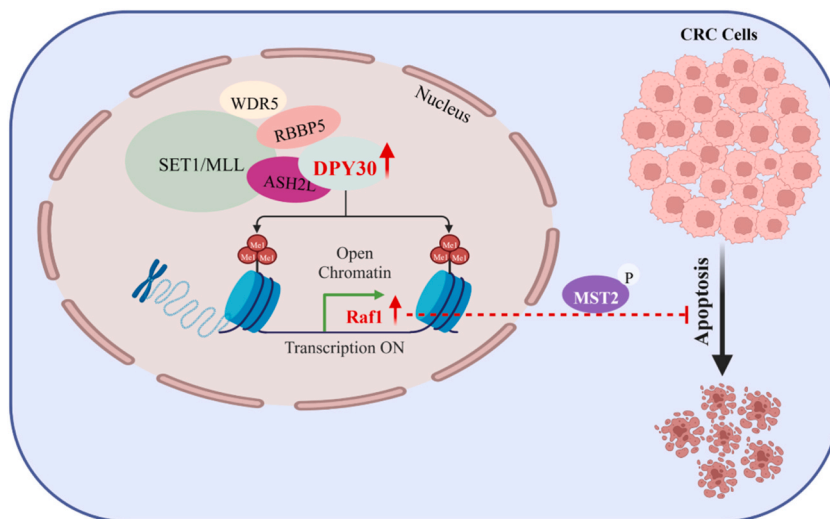

Fig. 7. Graphical Abstract. Schematic model showing the role of DPY30 in the regulation of CRC cells apoptosis. DPY30 knockdown may down-regulate histone H3K4me3 modification on Raf1 promoter and eventually promotes the apoptosis process of CRC cells.

Data availability

The data used and analyzed in the current study are available from the corresponding author upon a reasonable request.

Ethics approval

Our study was approved by the Ethics Committees of The First Affiliated Hospital of Xiamen University (Xiamen, China) (The IRB approval number: XMYY-2022KYSB097). Before tumor specimens obtained, they all under curative resection with informed consent and write informed consent at the Department of Colorectal Tumor Surgery, First Affiliated Hospital of Xiamen University. The animal procedures were approved by the Institutional Animal Care and Use Ethics Committee of Xiamen University and performed according to its regulations. We did our best to minimize animal suffering and undertaken according to the institution's guideline.

CRediT authorship contribution statement

HaiFeng Jiang: Writing – original draft, Investigation, Data curation. **WeiChao Su:** Writing – review & editing, Data curation. **HaiXing Wang:** Resources. **ChunYing Luo:** Data curation. **YaTao Wang:** Investigation. **LinJun Zhang:** Data curation. **LingTao Luo:** Resources. **ZeBin Lu:** Data curation. **DongYan Shen:** Writing – review & editing, Resources, Funding acquisition, Formal analysis, Conceptualization. **GuoQiang Su:** Writing – review & editing, Resources, Funding acquisition, Conceptualization.

Declaration of competing interest

The authors declare that they have no known competing financial interests or personal relationships that could have appeared to influence the work reported in this paper.

Appendix A. Supplementary data

Supplementary data to this article can be found online at https://doi.org/10.1016/j.heliyon.2024.e24807.

References

[1] H. Sung, J. Ferlay, R.L. Siegel, M. Laversanne, I. Soerjomataram, A. Jemal, F. Bray, Global cancer statistics 2020: GLOBOCAN estimates of incidence and mortality worldwide for 36 cancers in 185 countries, CA Cancer J Clin 71 (3) (2021) 209–249.

[2] J. Ferlay, I. Soerjomataram, R. Dikshit, S. Eser, C. Mathers, M. Rebelo, D.M. Parkin, D. Forman, F. Bray, Cancer incidence and mortality worldwide: sources, methods and major patterns in GLOBOCAN 2012, Int. J. Cancer 136 (5) (2015) E359–E386.

[3] Y. Zhang, Z. Chen, J. Li, The current status of treatment for colorectal cancer in China: a systematic review, Medicine (Baltim.) 96 (40) (2017) e8242.

[4] G. Tong, X. Wu, B. Cheng, L. Li, X. Li, Z. Li, Q. Nong, X. Chen, Y. Liu, S. Wang, Knockdown of HOXA-AS2 suppresses proliferation and induces apoptosis in colorectal cancer, Am J Transl Res 9 (10) (2017) 4545–4552.

[5] K. Tu, W. Yang, C. Li, X. Zheng, Z. Lu, C. Guo, Y. Yao, Q. Liu, Fbxw7 is an independent prognostic marker and induces apoptosis and growth arrest by regulating YAP abundance in hepatocellular carcinoma, Mol. Cancer 13 (2014) 110.

[6] Z. Liu, Y. Wang, C. Dou, M. Xu, L. Sun, L. Wang, B. Yao, Q. Li, W. Yang, K. Tu, et al., Hypoxia-induced up-regulation of VASP promotes invasiveness and metastasis of hepatocellular carcinoma, Theranostics 8 (17) (2018) 4649–4663.

[7] Q. Xu, J. Tu, C. Dou, J. Zhang, L. Yang, X. Liu, K. Lei, Z. Liu, Y. Wang, L. Li, et al., HSP90 promotes cell glycolysis, proliferation and inhibits apoptosis by regulating PKM2 abundance via Thr-328 phosphorylation in hepatocellular carcinoma, Mol. Cancer 16 (1) (2017) 178.

[8] J. Dabin, A. Fortuny, S.E. Polo, Epigenome maintenance in response to DNA damage, Mol. Cell 62 (5) (2016) 712–727.

[9] K.K. Li, C. Luo, D. Wang, H. Jiang, Y.G. Zheng, Chemical and biochemical approaches in the study of histone methylation and demethylation, Med. Res. Rev. 32 (4) (2012) 815–867.

[10] H. Jiang, The complex activities of the SET1/MLL complex core subunits in development and disease, Biochim Biophys Acta Gene Regul Mech 1863 (7) (2020) 194560.

[11] Y. Dou, T.A. Milne, A.J. Ruthenburg, S. Lee, J.W. Lee, G.L. Verdine, C.D. Allis, R.G. Roeder, Regulation of MLL1 H3K4 methyltransferase activity by its core components, Nat. Struct. Mol. Biol. 13 (8) (2006) 713–719.

[12] P. Ernst, C.R. Vakoc, WRAD: enabler of the SET1-family of H3K4 methyltransferases, Brief Funct Genomics 11 (3) (2012) 217–226.

[13] M.M. Steward, J.-S. Lee, A. O'Donovan, M. Wyatt, B.E. Bernstein, A. Shilatifard, Molecular regulation of H3K4 trimethylation by ASH2L, a shared subunit of MLL complexes, Nat. Struct. Mol. Biol. 13 (9) (2006) 852–854.

[14] A.J. Ruthenburg, C.D. Allis, J. Wysocka, Methylation of lysine 4 on histone H3: intricacy of writing and reading a single epigenetic mark, Mol. Cell 25 (1) (2007) 15–30.

[15] R. Rickels, A. Shilatifard, Enhancer logic and mechanics in development and disease, Trends Cell Biol. 28 (8) (2018) 608–630.

[16] H. Jiang, A. Shukla, X. Wang, Chen W-y, Bernstein BE, Roeder RG: role for Dpy-30 in ES cell-fate specification by regulation of H3K4 methylation within bivalent domains, Cell 144 (4) (2011) 513–525.

[17] Z. Yang, J. Augustin, C. Chang, J. Hu, K. Shah, C.-W. Chang, T. Townes, H. Jiang, The DPY30 subunit in SET1/MLL complexes regulates the proliferation and differentiation of hematopoietic progenitor cells, Blood 124 (13) (2014) 2025–2033.

[18] X. Wang, Z. Lou, X. Dong, W. Yang, Y. Peng, B. Yin, Y. Gong, J. Yuan, W. Zhou, M. Bartlam, et al., Crystal structure of the C-terminal domain of human DPY-30-like protein: a component of the histone methyltransferase complex, J. Mol. Biol. 390 (3) (2009) 530–537.

[19] J.F. Haddad, Y. Yang, Y.-H. Takahashi, M. Joshi, N. Chaudhary, A.R. Woodfin, A. Benyoucef, S. Yeung, J.S. Brunzelle, G. Skiniotis, et al., Structural analysis of the Ash2L/dpy-30 complex reveals a heterogeneity in H3K4 methylation, Structure 12 (2018) 26.

[20] R. Choudhury, S. Singh, S. Arumugam, A. Roguev, A.F. Stewart, The Set1 complex is dimeric and acts with Jhd2 demethylation to convey symmetrical H3K4 trimethylation, Genes Dev. 33 (9–10) (2019) 550–564.

[21] Z. Yang, K. Shah, A. Khodadadi-Jamayran, H. Jiang, Dpy30 is critical for maintaining the identity and function of adult hematopoietic stem cells, J. Exp. Med. 213 (11) (2016) 2349–2364.

[22] E. Simboeck, A. Gutierrez, L. Cozzuto, M. Beringer, L. Caizzi, W.M. Keyes, L. Di Croce, DPY30 regulates pathways in cellular senescence through ID protein expression, EMBO J. 32 (16) (2013) 2217–2230.

[23] Y.J. Lee, M.-E. Han, S.-J. Baek, S.-Y. Kim, S.-O. Oh, Roles of DPY30 in the proliferation and motility of gastric cancer cells, PLoS One 7 (2015) e0131863, 10.

[24] L. Zhang, S. Zhang, A. Li, A. Zhang, S. Zhang, L. Chen, DPY30 is required for the enhanced proliferation, motility and epithelial-mesenchymal transition of epithelial ovarian cancer cells, Int. J. Mol. Med. 42 (6) (2018) 3065–3072.

[25] F.-X. He, L.-L. Zhang, P.-F. Jin, D.-D. Liu, A.-H. Li, DPY30 regulates cervical squamous cell carcinoma by mediating epithelial-mesenchymal transition (EMT), OncoTargets Ther. 12 (2019) 7139–7147.

[26] Z.-F. Hong, W.-Q. Zhang, S.-J. Wang, S.-Y. Li, J. Shang, F. Liu, D.-Y. Shen, Upregulation of DPY30 promotes cell proliferation and predicts a poor prognosis in cholangiocarcinoma, Biomedicine & Pharmacotherapy = Biomedecine & Pharmacotherapie 123 (2020) 109766.

[27] W.-C. Su, X.-M. Mao, S.-Y. Li, C.-Y. Luo, R. Fan, H.-F. Jiang, L.-J. Zhang, Y.-T. Wang, G.-Q. Su, D.-Y. Shen, DPY30 promotes proliferation and cell cycle progression of colorectal cancer cells via mediating H3K4 trimethylation, Int. J. Med. Sci. 20 (7) (2023) 901–917.

[28] D. Ribble, N.B. Goldstein, D.A. Norris, Y.G. Shellman, A simple technique for quantifying apoptosis in 96-well plates, BMC Biotechnol. 5 (2005) 12.

[29] E. O'Neill, W. Kolch, Taming the Hippo: raf-1 controls apoptosis by suppressing MST2/Hippo, Cell Cycle 4 (3) (2005) 365–367.

[30] H. Brenner, M. Kloor, C.P. Pox, Colorectal cancer, Lancet 383 (9927) (2014) 1490–1502.

[31] Y. Okugawa, W.M. Grady, A. Goel, Epigenetic alterations in colorectal cancer: emerging biomarkers, Gastroenterology 5 (2015) 149.

[32] G. Jung, E. Hernández-Illán, L. Moreira, F. Balaguer, A. Goel, Epigenetics of colorectal cancer: biomarker and therapeutic potential, Nat. Rev. Gastroenterol. Hepatol. 17 (2) (2020) 111–130.

[33] D. Dixit, B.C. Prager, R.C. Gimple, T.E. Miller, Q. Wu, S. Yomtoubian, R.L. Kidwell, D. Lv, L. Zhao, Z. Qiu, et al., Glioblastoma stem cells reprogram chromatin in vivo to generate selective therapeutic dependencies on DPY30 and phosphodiesterases, Sci. Transl. Med. 626 (2022) 14, eabf3917.

[34] R. Ivey, M. Desai, K. Green, I. Sinha-Hikim, T.C. Friedman, A.P. Sinha-Hikim, Additive effects of nicotine and high-fat diet on hepatocellular apoptosis in mice: involvement of caspase 2 and inducible nitric oxide synthase-mediated intrinsic pathway signaling, Horm. Metab. Res. 46 (8) (2014) 568–573.

[35] D. Kashyap, H.S. Tuli, M.B. Yerer, A. Sharma, K. Sak, S. Srivastava, A. Pandey, V.K. Garg, G. Sethi, A. Bishayee, Natural product-based nanoformulations for cancer therapy: opportunities and challenges, Semin. Cancer Biol. (2021) 69.

[36] P. Noble, M. Vyas, A. Al-Attar, S. Durrant, J. Scholefield, L. Durrant, High levels of cleaved caspase-3 in colorectal tumour stroma predict good survival, Br. J. Cancer 108 (10) (2013) 2097–2105.

[37] Q. Yang, W. Jiang, P. Hou, Emerging role of PI3K/AKT in tumor-related epigenetic regulation, Semin. Cancer Biol. 59 (2019) 112–124.

[38] J.M. Spangle, T.M. Roberts, J.J. Zhao, The emerging role of PI3K/AKT-mediated epigenetic regulation in cancer, Biochim. Biophys. Acta Rev. Canc 1868 (1) (2017) 123–131.

[39] Y. Han, Y. Peng, Y. Fu, C. Cai, C. Guo, S. Liu, Y. Li, Y. Chen, E. Shen, K. Long, et al., MLH1 deficiency induces cetuximab resistance in colon cancer via her-2/PI3K/AKT signaling, Adv. Sci. 7 (13) (2020) 2000112.

[40] G. Cheng, F. An, Z. Cao, M. Zheng, Z. Zhao, H. Wu, DPY30 promotes the growth and survival of osteosarcoma cell by regulating the PI3K/AKT signal pathway, Eur. J. Histochem. 1 (2023) 67.

[41] E.J. Sun, M. Wankell, P. Palamuthusingam, C. McFarlane, L. Hebbard, Targeting the PI3K/Akt/mTOR pathway in hepatocellular carcinoma, Biomedicines 11 (2021) 9.

[42] M. Yu, B. Qi, W. Xiaoxiang, J. Xu, X. Liu, Baicalein increases cisplatin sensitivity of A549 lung adenocarcinoma cells via PI3K/Akt/NF-kappaB pathway, Biomed. Pharmacother. 90 (2017) 677–685.

[43] H. Chen, L. Zhou, X. Wu, R. Li, J. Wen, J. Sha, X. Wen, The PI3K/AKT pathway in the pathogenesis of prostate cancer, Front. Biosci. 21 (5) (2016) 1084–1091.

[44] M.M. Brune, D. Juskevicius, J. Haslbauer, S. Dirnhofer, A. Tzankov, Genomic landscape of hodgkin lymphoma, Cancers 4 (2021) 13.

[45] J. Wang, S. Liu, T. Heallen, J.F. Martin, The Hippo pathway in the heart: pivotal roles in development, disease, and regeneration, Nat. Rev. Cardiol. 15 (11) (2018) 672–684.

[46] M. Radu, J. Chernoff, The DeMSTification of mammalian Ste 20 kinases, Curr. Biol. 19 (10) (2009) R421–R425.

[47] J.D. Graves, Y. Gotoh, K.E. Draves, D. Ambrose, D.K. Han, M. Wright, J. Chernoff, E.A. Clark, E.G. Krebs, Caspase-mediated activation and induction of apoptosis by the mammalian Ste 20-like kinase Mst1, EMBO J. 17 (8) (1998) 2224–2234.

[48] J.D. Graves, K.E. Draves, Y. Gotoh, E.G. Krebs, E.A. Clark, Both phosphorylation and caspase-mediated cleavage contribute to regulation of the Ste 20-like protein kinase Mst1 during CD95/Fas-induced apoptosis, J. Biol. Chem. 276 (18) (2001) 14909–14915.

[49] H. Glantschnig, G.A. Rodan, A.A. Reszka, Mapping of MST1 kinase sites of phosphorylation. Activation and autophosphorylation, J. Biol. Chem. 277 (45) (2002) 42987–42996.

[50] W.L. Cheung, K. Ajiro, K. Samejima, M. Kloc, P. Cheung, C.A. Mizzen, A. Beeser, L.D. Etkin, J. Chernoff, W.C. Earnshaw, et al., Apoptotic phosphorylation of histone H2B is mediated by mammalian sterile twenty kinase, Cell 113 (4) (2003) 507–517.